Proceedings of the 28th IEEE
EMBS Annual International Conference
New York City, USA, Aug 30-Sept 3, 2006

A wavefront-based constraint for potential surface solutions in inverse electrocardiography

Alireza Ghodrati, Andrew Keely, Gilead Tadmor, Rob MacLeod, and Dana H. Brooks

Abstract— **Inverse electrocardiography in recent years has generally been approached using one of two quite distinct source models, either a potential-based approach or an activation-based approach. Each approach has advantages and disadvantages relative to the other, which are inherited by all specific methods based on a given approach. Recently our group has been working to develop models which can bridge between these two approaches, hoping to capture some of the most important advantages of both. In this work we present one such effort, which we term wavefront-based potential reconstruction (WBPR). It is a modification of standard regularization methods for potential-based inverse electrocardiography, into which we incorporate a constraint based on a wavefront-like approximation to the potential-based solution. Initial results indicate significant improvement with respect to localization and characterization of the wavefront in simulations using both epicardially and supra-ventricularly paced heartbeats.**

I. Introduction

Inverse electrocardiography is a noninvasive imaging method to reconstruct the heart's electrical activity from surface measurements. Recent reports indicate great potential for this imaging modality to be used in clinical practice for cardiac electrophysiology and arrhythmias [1, 2]. Inverse electrocardiography in recent years has generally been approached using one of two quite distinct source models, either a potential-based approach or an activation-based approach. (For representative examples of each see [1, 3–7] and [2, 8–11] respectively.) For example, activation-based approaches use a much more parsimonious representation which nonetheless captures the the single most important physiological feature of cardiac propagation. However they generally employ simplifying assumptions which may make it impossible to reconstruct localized features such as diminished height of the wavefront and decreased slope of the intrinsic deflection. Moreover any aspect of cardiac electrical behavior outside of activation (or, in some generalizations, recovery) are simply not included in the model. Potential-based approaches are high-order parameterizations which can accommodate a broad range of possible phenomena. However they are much more ill-conditioned than activation-based models, requiring considerable regularization. It has proved difficult to impose regularizing constraints which directly capture physiology. Moreover these models have been reported to be considerably less robust than activation-based models to uncertainty in the internal torso geometry [12].

Recently our group has been working to develop models which can bridge between these two approaches, hoping to capture some of the most important advantages of both. Such models should try to maintain the low dimensionality implied by a focus on wavefront behavior, but should relax the isotropy and homogeneity assumptions of activation models, and should also seek to permit inclusion of relevant physiology and electrophysiology. We have developed two such models, which we call wavefront-based curve reconstruction (WBCR) and wavefront-based potential reconstruction (WCPR) [13, 14]. The WBCR method reconstructs an activation curve at each time instant using a state evolution approach. In this work we concentrate on the WBPR method. It is a modification of standard regularization methods for potential-based inverse electrocardiography, into which we incorporate a constraint based on a wavefront-like approximation to the potential-based solution. The procedure is carried out in a time-recursive fashion, with the solution used from the previous time instant used to create the wavefront-based constraint for the next time instant. We also show how this approach can be re-interpreted in statistical regularization terms as an estimate of the mean of a prior density. Initial results indicate significant improvement with respect to localization and characterization of the wavefront in simulations using both epicardially and supra-ventricularly paced heartbeats.

II. Wavefront-based potential reconstruction (WBPR)

The WBPR method depends on the construction and use, at each time instant, of an "initial guess", or comparison constraint, or mean of a prior, based on a highly quantized approximation of the potential surface. Specifically, this approximation allows only two values of the potential far from the wavefront; zero (or in practice a time-varying reference value, see below) in unactivated regions, and a fixed negative potential (again with the addition of the time-varying reference) in regions through which the wavefront has passed. In between these two spatially constant regions the approximation places a relatively sharp interpolated transition region, using a fixed functional relationship to determine the interpolation. The reference potential drift, which shifts this two level image, increases over time proportionally to the area of the activated region [15]. As described above, this two-level model is used as an initial estimate, or prior mean, and then updated using the body surface measurements and the forward model.

The specific model used for the transition region is given as follows:

1-4244-0033-3/06/$20.00 ©2006 IEEE.

$$\overline{x}_{k,i} = \alpha_{k,i}\frac{V}{2}(1 - e^{-0.5d_{k,i}}) - \frac{V}{2} + V_{\mathrm{ref}_k}, \qquad (1)$$

where $\overline{x}_{k,i}$ is the potential estimate of the i^{th} node at time instant k, $\alpha_{k,i}$ is -1 or 1 depending on whether the i^{th} node is inside or outside the wavefront, respectively, V is the pre-determined wavefront height, $d_{k,i}$ is the distance of the i^{th} node to the wavefront curve at time instant k and V_{ref_k} is the potential reference at time instant k. The wavefront location at time k is defined as the location of the iso-potential contour whose value is the average of the two levels, $(-V + V_{\mathrm{ref}_k})/2$.

We then use the resulting approximation surface as an initial solution in a deterministic Tikhonov regularization. (We discuss a statistical interpretation of the method below.) The Tikhonov (sometimes called Twomey) [16], solution in the presence of an initial estimate at time instant k, was obtained by minimizing

$$J_k = ||\mathbf{A}\mathbf{x_k} - \mathbf{y_k}||_2^2 + \lambda^2||\mathbf{x_k} - \overline{\mathbf{x}}_\mathbf{k}||_2^2, \qquad (2)$$

where $\mathbf{y_k}$ are the potential measurements on the torso at time instant k, $\mathbf{A}$ is the forward matrix, $\mathbf{x_k}$ holds the heart surface potentials at time instant k, λ is the regularization parameter and $\overline{\mathbf{x}}_\mathbf{k}$ is the initial wavefront-based estimate as described by Eq. 1.

The inverse solution obtained from the minimization of J_k follows:

$$\widehat{\mathbf{x}}_\mathbf{k} = \overline{\mathbf{x}}_\mathbf{k} + (\mathbf{A^T A} + \lambda^2\mathbf{I})^{-1}\mathbf{A^T}(\mathbf{y_k} - \mathbf{A}\overline{\mathbf{x}}_\mathbf{k}). \qquad (3)$$

Viewed as a spatial-temporal process, a wavefront contour estimated from the solution for the potentials at the previous time instant, after some smoothing, was used to calculate the wavefront-shaped model of the potentials at the current time instant. Thus the inverse solution $\widehat{\mathbf{x}}_\mathbf{k}$ was be obtained in a temporally recursive fashion as follows:

$$\begin{array}{ll} \text{Step 1}: & \mathbf{c_k} = \mathbf{h}(\widehat{\mathbf{x}}_{\mathbf{k-1}}) \\ \text{Step 2}: & \overline{\mathbf{x}}_\mathbf{k} = \mathbf{g}(\mathbf{c_k}) \\ \text{Step 3}: & \text{Calculate } \widehat{\mathbf{x}}_\mathbf{k} \text{ using Eq. (3)} \end{array}, \qquad (4)$$

where $\widehat{\mathbf{x}}_\mathbf{k}$ is our solution for the potentials at time k, $\mathbf{c_k}$ is an interpolated continuous curve representing the k'th position of the wavefront, $\mathbf{h}()$ finds this wavefront curve by thresholding the potential and then using cubic B-splines to smooth the threshold contour, and $\mathbf{g}()$ is the potential function of Eq. (1).

A. Implementation

As noted above, to start the method we need

- the value of the reference at each time instant,
- the negative value of the activated region of any single time instant and the fixed height of the wavefront, and
- an initial position for the wavefront.

In the simulations presented here we obtained these values as follows:

We simply used the true value of the negative potential of the activated region based on actual measurements, although.based on results in [17, 18] we believe that it should be possible to estimate this value with reasonable accuracy using the Tikhonov solution at a node far from the wavefront. The initial value of the reference potential was taken as zero (a correct assumption for early in QRS). The subsequent values of the reference with a one time sample lag were extracted sequentially from the inverse solution at each time instant. We used the potential of the last lead to be activated as the reference drift in the first half of the QRS interval and the shift of the earliest activating node potential from its starting point as the reference drift in the second half. The initial wavefront estimate was taken as a circular wavefront centered at the pacing node, with a radius of about 2cm. We assumed that the pacing node was known, but again there is evidence to suggest that it could be obtained reliably enough for this purpose (with around 2cm uncertainty) by a standard Tikhonov solution or perhaps a GMRES approach [6].

The threshold function $\mathbf{h}()$ was implemented by checking all the triangles of the heart surface triangular mesh locate triangles which contained the wavefront. Through linear interpolation along the triangle edges we approximated the wavefront crossing points. The result was a pair of points on the wavefront on two sides of each triangle through which the wavefront passed. Since neighboring triangles which contained the wavefront shared one of these points, we started from an arbitrary pair of points, found the neighboring triangles, and continued in this manner until we reached the starting point. We looked for multiple wavefront curves, using the above procedure to locate all of them. Finally, we downsampled the curve points and used a cubic B-spline basis to interpolate the wavefront curve or curves. Function $\mathbf{g}()$ was implemented based on Eq. (1) and the distance from node i to the wavefront, $d_{k,i}$, was approximated using a spherical arc approximation.

In summary, at each time instant we found the wavefront corresponding to the threshold potential solution of the previous time instant, smoothed by a cubic B-spline fit, then used this smoothed wavefront to create an initial estimate for the current time instant. This initial estimate was then used as the constraint in a Tikhonov solution as per Eq. (3). We also implemented the method iterating backwards in time.

III. Results

We tested the method using canine epicardial potentials measured in a tank built to simulate an adolescent human torso at the CVRTI. Measurements were taken at 490 sites on the heart surface using a sock electrode as described elsewhere [19]. Our forward matrix was calculated using the Boundary Element Method to with 771 nodes on the torso mesh. Testing of the methods was always performed on data from different animals than those used to estimate the model parameters. To test the inverse solution we simulated torso measurements from the measured heart data using the forward matrix and then added white Gaussian noise at an SNR of 30dB.

Fig. 1 shows potential maps for an supra-ventricularly paced heart beat, along with inverse solutions obtained by the WBPR approach (forward and backward), and the standard

zero-order Tikhonov solution, at selected time instants. We report this example because the existence of multiple, separate activation regions are more challenging for the WBPR method. All the images in each row have the same mapping from value to gray shade and the contours show the isopotential lines. The left column shows an electrogram from a point close to first epicardial breakthrough site, and the time indicated on each row is with respect to the breakthrough time. The plots were drawn with *map3d* software [20]. We also calculated the relative error norm (RE) as $\mathrm{RE} = ||\mathbf{x} - \hat{\mathbf{x}}||/||\mathbf{x}||$, where $\mathbf{x}$ and $\hat{\mathbf{x}}$ represent the experimental data and inverse solution respectively. Fig. 2 shows the RE value versus time for the Tikhonov, WBPR forward and WBPR backward inverse solutions for both this beat and a left-ventricle paced beat.

The results showed that reconstructed solutions using the proposed method were considerably improved over the Tikhonov solutions. At early time instants ($t = 2$), the backward iterations reconstructed the potential map and wavefront location quite accurately to the experimental data. Later ($t = 9$), a second breakthrough appeared on the apex which the WBPR method was captured more accurately than the Tikhonov solution. At the later time instants shown, the Tikhonov solution was very broad and smooth while the WBPR solutions much more clearly reflected the presence of a narrow wavefront found in the experimental data. Interestingly, the RE figures for this latter time instant do not reflect this difference. The lower panel of Fig. 2 shows RE values as a function of time for this beat; for both beats shown in this figure we note that the forward prediction method did better in the second half of QRS while the backwards method generally did better early in the beat only.

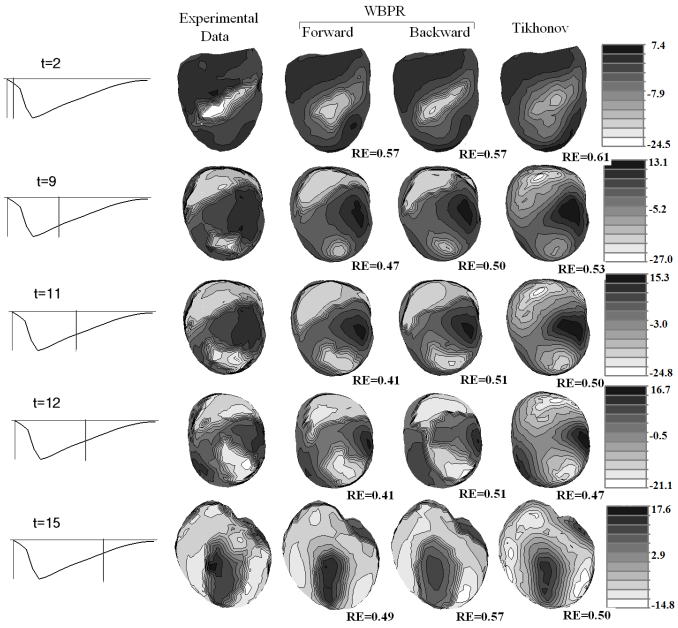

Fig. 1. potential map of the experimental data along with the solutions of WBPR approach (forward and backward) and Tikhonov for an atrial drive paced heart beat. The parameter t shows the time in ms with respect to first breakthrough on the epicardial surface. The left column shows the time signal of a point close to the pacing site. Relative error norm (RE) of each inverse solution is shown under corresponding potential map.

IV. Discussion

Considerable previous research in inverse electrocardiography has focused on using an appropriate covariance matrix (regularization matrix) to improve the inverse solution while the mean was assumed to be zero [21]. Other work which used an initial estimate of the solution to add temporal information used the Tikhonov solution [16]. In a statistical context, in the work described above the wavefront-based constraint $\overline{\mathbf{x}}_\mathbf{k}$ plays the role of the mean of a prior density and the covariance matrix is taken as a scalar times the identity, i.e uncorrelated epicardial potentials. We tested the WBPR method incorporating a structured covariance matrix estimate; we estimated this covariance matrix as a diagonal matrix whose diagonal elements were a function of the distance of corresponding nodes on the heart surface to the wavefront, so that we placed more confidence in the estimated mean farther from the wavefront and less confidence in its vicinity. Somewhat surprisingly, simulation results showed little improvement when this covariance matrix replaced the simple uncorrelated assumption. This suggest that previous neglect of the value of the mean in statistical approaches may have been a source of considerable error. One approach which could be considered would be to combine the mean estimator with a spatio-temporally derived estimate of the covariance matrix, for instance using an approach based on the isotropy assumption as proposed in [22]. The zero-order temporal predictor of the wavefront location in the current WBPR approach might also be improved by substitution of a more sophisticated model.

In certain conditions, such as ischemia or post-infarction, the height of the wavefront changes on the heart. Activation-based methods tend to have difficulty with this problem [7]. The WBPR approach does not impose a strictly-determined wavefront height. In the current implementation of this method we found the wavefront from the estimated potentials by thresholding, assumed the wavefront curve was located at the mid-points of a fixed-height (20mv) wavefront transition region. Therefore, in conditions such as ischemia or post-infarction, careful attention may be required to the thresholding, and perhaps even an adaptive technique might need to be employed to detect the wavefront from the estimated potentials.

Although we report RE values as a metric for assessing the accuracy of the WBPR method, as noted in Sec. III the RE values at times did not correspond well to visual, i.e. qualitative, assessment of wavefront reconstruction, especially later in QRS. More comprehensive assessment of accuracy of wavefront reconstruction in WBPR requires the development and testing of new and appropriate metrics. Space precludes presentation of these developments here but they will be included in our presentation at the conference.

More generally, a more comprehensive comparison of both WBPR and WBCR methods with other, both activation and potential-based methods, requires the development of a testbed platform which includes both endocardial and

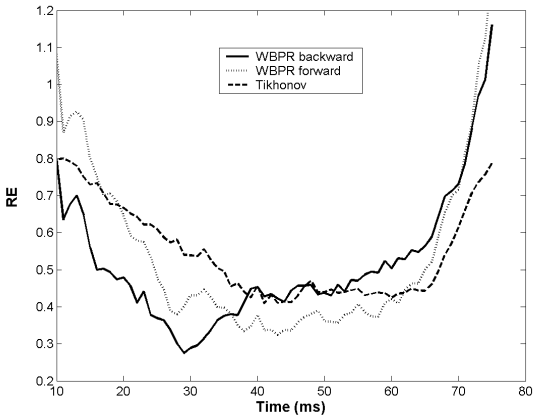

(a)

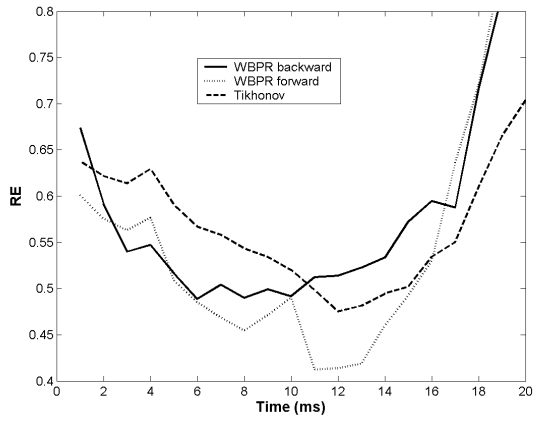

(b)

Fig. 2. Relative error norm (RE) versus time (with respect to the pacing time) in ms for (a) left ventricle paced and (b) supraventricular paced heart beats.

epicardial surfaces. Technical limitations of our apparatus at CVRTI has impeded such development to date. However we are actively pursuing several directions towards creation of such a testbed, and we will present such comparisons at the conference.

Finally, robustness to error in the forward model is not reported on here. It is reasonable to expect that the use of a wavefront-based constraint, along with careful estimation of the reference drift, should retain some of the robustness to this error shown by activation-based methods; however this clearly needs to be investigated. Using the combined epi/endocardial surface model we will soon be able to test this hypothesis.

ACKNOWLEDGMENT

The authors are indebted to Bruno Taccardi and Bonnie Punske for their advice, encouragement, and critical comments on our work. This work was supported in part by the National Institutes of Health, National Center for Research Resources, grant number 1-P41-RR12553-3.

REFERENCES

[1] C. Ramanathan, R. N. Ghanem, P. Jia1, K. Ryu, and Y. Rudy, "Noninvasive electrocardiographic imaging for cardiac electrophysiology and arrhythmia," *Nature Medicine*, vol. 10, pp. 422–428, 2004.

[2] B. Tilg, G. Fischer, R. Modre, F. Hanser, B. Messnarz, M. Schocke, C. Kremser, T. B. F. Hintringer, and F. Roithinger, "Model-based imaging of cardiac electrical excitation in humans," *IEEE Trans. Med. Imaging*, vol. 21, no. 9, pp. 1031–1039, Sept. 2002.

[3] D. H. Brooks, G. F. Ahmad, R. S. MacLeod, and G. M. Maratos, "Inverse electrocardiography by simultaneous imposition of multiple constraints," *IEEE Trans Biomed. Eng.*, vol. 46, no. 1, pp. 3–18, 1999.

[4] F. Greensite and G. Huiskamp, "An improved method for estimating epicardial potentials from the body surface," *IEEE Trans. Biomed. Eng.*, vol. 45, pp. 98–104, 1998.

[5] A. van Oosterom, "The use of spatial covariance in computing pericardial potentials," *IEEE Trans Biomed. Eng.*, vol. 46, no. 7, pp. 778–787, 1999.

[6] C. Ramanathan, P. Jia, R. Ghanem, D. Calvetti, and Y. Rudy, "Noninvasive electrocardiographic imaging (ECGI): application of the generalized minimal residual (GMRes) method." *Annal. Biomed. Eng.*, vol. 31, no. 8, pp. 981–994, Sep 2003.

[7] B. Messnarz, B. Tilg, R. Modre, G. Fischer, and F. Hanser, "A new spatiotemporal regularization approach for reconstruction of cardiac transmembrane potential patterns," *IEEE Trans Biomed. Eng.*, vol. 51, no. 2, pp. 273–281, Feb. 2004.

[8] J. Cuppen and A. van Oosterom, "Model studies with the inversely calculated isochrones of ventricular depolarization," *IEEE Trans Biomed. Eng.*, vol. 31, pp. 652–659, 1984.

[9] G. Huiskamp and A. van Oosterom, "The depolarization sequence of the human heart surface computed from measured body surface potentials," *IEEE Trans Biomed. Eng.*, vol. 35, pp. 1047–1059, 1989.

[10] G. J. Huiskamp and F. Greensite, "A new method for myocardial activation imaging," *IEEE Trans Biomed. Eng.*, vol. 44, pp. 433–446, 1997.

[11] A. J. Pullan, L. K. Cheng, M. P. Nash, C. P. Bradley, and D. J. Paterson, "Noninvasive electrical imaging of the heart: Theory and model development," *Annals of Biomed. Eng.*, vol. 29, pp. 817–836, 2001.

[12] L. K. Cheng, J. M. Bodley, and A. J. Pullan, "Effects of experimental and modeling errors on electrocardiographic inverse formulations," *IEEE Trans Biomed. Eng.*, vol. 50, no. 1, pp. 23–32, Jan. 2003.

[13] A. Ghodrati, D. Brooks, G. Tadmor, B. Punske, and R. MacLeod, "Wavefront-based inverse electrocardiography using an evolving curve state vector and phenomenological propagation and potential models," in *c-BEMNFSI2005*, Minn, MN, May 2005.

[14] A. Ghodrati, D. Brooks, G. Tadmor, and R. MacLeod, "Wavefront-based models for inverse electrocardiography," *IEEE Trans Biomed. Eng.*, vol. in press, 2006.

[15] B. Punske, R. Lux, R. MacLeod, P. Ershler, T. Dustman, Y. Vyhmeister, and B. Taccardi, "Experimental study and removal of the drift of the reference potential from the unipolar electrogram," in *Proceedings of The First Joint BMES/EMBS Conference*, IEEE EMBS & MBES. IEE Press, 1999, p. 303.

[16] H. S. Oster and Y. Rudy, "The use of temporal information in the regularization of the inverse problem of electrocardiography," *IEEE Trans. Biomed. Eng.*, vol. 39, pp. 65–75, 1992.

[17] J. Burns, B. Taccardi, R. MacLeod, and Y. Rudy, "Noninvasive electrocardiographic imaging of electrophysiologically abnormal substrates in infarcted hearts: A model study," *Circ.*, vol. 101, pp. 533–540, 2000.

[18] J. Burnes, B. Taccardi, and Y. Rudy, "A noninvasive imaging modality for cardiac arrhythmias," *Circ.*, vol. 102, pp. 2152–2158, 2000.

[19] R. MacLeod, Q. Ni, B. Punske, P. Ershler, B. Yilmaz, and B. Taccardi, "Effects of heart position on the body-surface ECG," *J. of Electrocardiology*, vol. S33, pp. 229–237, 2000.

[20] R. MacLeod and C. Johnson., "Map3d: Interactive scientific visualization for bioengineering data," in *IEEE Engineering in Medicine and Biology Society 15th Annual International Conference*. IEEE press, 1993, pp. pages 30–31.

[21] A. van Oosterom, "The spatial covariance used in computing the pericardial potential distribution," in *Computational Inverse Problems in Electrocardiography*, P. R. Johnston, Ed. Southampton, UK: WITpress, 2001, pp. 1–50.

[22] F. Greensite, "The temporal prior in bioelectromagnetic source imaging problems," *IEEE Trans Biomed. Eng.*, vol. 50, pp. 1152–1159, 2003.